In-Space Propellant Acquisition with Pleated Screen Tubes

S. Boraas* and A.J. LaBruna†
Textron Bell Aerospace, Buffalo, N.Y.

It is shown that a device consisting of multiple-screen tubes located around the periphery of a cylindrical tank can be an effective means of acquiring propellant. A major part of this study dealt with the development of analytical methods for determining the feasibility of the multiple-tube arrangement and the application of these methods in the calculation of its performance in a compartmented tank. The initial analysis confirmed the feasibility from the standpoint of expulsion efficiency. Lacking knowledge on the nature of the incoming velocity at the surface of a porous tube closed at one end, a uniform velocity distribution was assumed in the calculation of the corresponding flow pressure drop. Subsequently, a mathematical model of the flow through the tube was developed, based upon a more realistic exponential distribution. Tests with a single tube using water and Freon T.F. verified the exponential distribution. Additional tests simulating space expulsion from a cylindrical tank were conducted using a four-tube acquisition device. Performed in both the horizontal and vertical attitudes, the latter tests indicated that high expulsion efficiencies could be expected if the multiple-tube acquisition device were used in a propellant tank onboard a space vehicle.

Nomenclature

a = ratio of local to standard acceleration
c_1, c_2 = constants
d_h = diameter of holes in support tube
d_p = outer diameter of pressure probe
d_S = mean diameter of pleated screen tube
d_T = outer diameter of support tube
D = tank diameter
EF = expulsion factor
h = height
k = screen resistance coefficient
ℓ = liquid immersed length of tube
ℓ_S = effective screen length of pleated screen tube
L = tank length
m,n = exponential constants
N = number of holes per unit length in support tube
N_{nf} = number of nonflowing screen tubes
N_T = total number of screen tubes
p = static pressure
P = total pressure
ΔP = pressure loss
ΔP_{bp} = bubble point value of screen
q = dynamic pressure
r = radial coordinate measured from tube centerline
t = thickness
u = internal flow velocity at open end of tube
U = centerline flow velocity at open end of tube
$\dot{w}$ = total flow rate
x = axial coordinate along tube
α = screen area multiplication factor due to pleating
β = inclination angle of tube relative to gas-propellant interface
δ = tube-tank wall spacing
ρ = propellant density
ϕ = screen porosity (ration of void volume to bulk volume)
ψ = angle defined in Fig. 5

Subscripts

cb = composite boundary
c = closed end of tube
f = friction loss
g = pressurant gas
max = maximum
min = minimum
s = screen
S = screen tube
tf = turning friction loss
tm = turbulent mixing loss
T = support tube

Superscripts

= nondimensional distance, axial divided by ℓ_S and radial by $2/(d_T - 2t_T)$
= average value

I. Introduction

In recent years, increased interest has been shown in liquid propellant tank systems in which devices using the surface tension energy of the propellant either retain or acquire propellant in a low acceleration environment. These include single or multiple arrangements of screens, capillary tubes, baffles, liners, and galleries.[1-3]‡ In a recent study at Bell Aerospace, an arrangenent of multiple pleated screen tubes was shown to have a real potential as an in-space propellant acquisition device. Shown in Fig. 1, the pleated screen tube was chosen as a basic component for the following reasons: a) the local acquisition capability of a tube provides greater flexibility in designing for specific mission requirements, for example, the extremely high launch accelerations of a strategic missile followed by deployment maneuvers, b) the ability to design for dynamic stability so as to avoid a decrease in expulsion efficiency due to meniscus failure in a vibration environment, c) the exploitation of a well developed commercial fabrication method, used by the filter industry in making similar tubes, to provide a low cost design approach to a surface tension management system, d) the pleating adds additional flow entrance area, which was believed to be important in achieving a high expulsion efficiency.

Presented as Paper 74-1152 at the AIAA/SAE 10th Propulsion Conference, San Diego, California, October 21-23, 1974; submitted November 1, 1974; revision received September 22, 1975.
Index category: Spacecraft Ground Testing and Simulation (Including Components).
*Principal Engineer. Member AIAA.
†Project Engineer.
‡Recent references only.

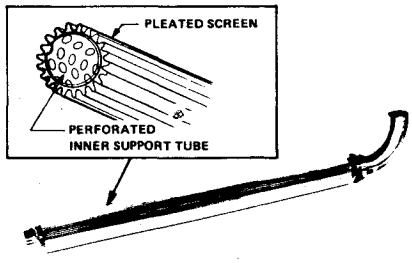

Fig. 1 Pleated screen tube.

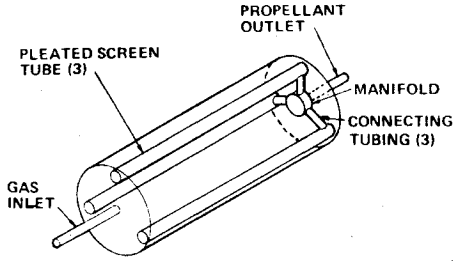

Fig. 2 Schematic of screen tube acquisition device.

An analysis to determine the expulsion efficiency of the multiple tube device in a tank oriented both horizontally and vertically proved its feasibility. In this analysis, which was limited to a cylindrical tank for which the device is specifically adapted, the total pressure drop attributable to the flow through a tube was unknown; therefore, it was estimated on the basis of an assumed uniform velocity distribution along the tube. Because we felt that a more exact determination of this pressure loss would be necessary in determining the capability of the device to deliver gas-free propellant, a mathematical model for computing this loss was developed. The development of this model, along with the expulsion analysis, comprised a major portion of the work conducted during this program.

The results of a 1g test program using water and Freon T.F. verified the velocity distribution calculated from the mathematical model. A four-tube acquisition device was assembled and water flow tested in a cylindrical tank in both the horizontal and vertical attitudes. Simulating expulsion of N_2O_4 under space conditions, these tests demonstrated that high expulsion efficiencies would be possible in a space application of this acquisition device.

II. Analyses

Several analytical studies were made in the evaluation of the multiple tube concept. The first analysis consisted of determining its expulsion efficiency in a cylindrical tank as a function of tank diameter, number and diameter of tubes, tank orientation relative to the acceleration vector, and total propellant flow rate. These calculations required the determination of the total flow pressure drop through the tubes and the adjoining hardware. The portion of this loss contributed by the tubing connecting the screen tubes was readily calculated. The remaining part, which is the loss through the tubes themselves, was computed after neglecting the internal losses, assuming a uniform velocity distribution and assuming this loss to be that incurred by the flow in passing through the screen. A subsequent analysis consisted in the development of a mathematical model for more precisely calculating this tube pressure drop. These analyses are described in more detail in the following paragraphs.

Expulsion Efficiency

The expulsion efficiency of a multiple screen tube acquisition device was calculated. Expressed as an expulsion factor (EF), it is defined as the ratio of the quantity of liquid expelled from the tank to the total tank volume.

All efficiencies were computed on the assumption of a cylindrical tank in which the screen tubes were assumed to be equally spaced around the periphery and to be of the same length as the tank. Figure 2 is a schematic of a three-tube device, along with the connecting tubing and a common manifold. In these calculations, the total volume associated with the screen material was assumed negligible; only the volume of the perforated inner support tube of the screen tube was considered.

Nonflowing Case

Calculation of the expulsion efficiency for the nonflowing case is an exercise in geometrically determining the amount of unobtainable propellant in the tank when the acceleration vector is perpendicular to the tank centerline and bisects the angle between any two adjacent tubes. This would be a worst case condition. Figure 3 is an end view of a tank (with a four-tube device) under those conditions where the cross hatched areas represent the irretrievable propellant. From the geometry of these areas, the expulsion factor is

$$EF = 1 - \left\{ \frac{4\delta(D-\delta)}{N_T D^2} + \left[1 - \frac{2\delta}{D}\right]\left[\frac{1}{N_T} - \frac{1}{2\pi}\sin\left[\frac{2\pi}{N_T}\right]\right] + N_T\left[\left[\frac{d_S}{D}\right]^2 - \frac{4t_T}{D^2}\left[d_T - t_T - \frac{Nd_h^2}{4}\right]\right]\right\} \quad (1)$$

where, for a given size and number of tubes, the tube-tank wall spacing δ must be such that high expulsion efficiencies are possible. A mathematical model of the liquid fillet configuration in this spacing at near empty tank conditions was also developed, using the minimum surface energy principle. Corroborated by neutral buoyancy tests, it permitted a more judicious selection for a value for δ.

Programmed for computer calculation, Eq. (1) was used to compute the expulsion factors for a nominal size tank, using N_2O_4. The results shown in Fig. 4 as an expulsion efficiency are expressed in terms of the number and the mean screen diameter of the tubes. The dashed line is a locus of points representing the maximum number of tubes that can be placed around the tank periphery. As indicated, the maximum expulsion efficiency is a fairly well defined point on these curves, especially at the larger tube diameters. For example, a mean screen diameter of 2.00 in. gives a maximum expulsion efficiency of 94.7% with a total of eight tubes. These results, although computed under a no-flow condition, do represent the near limiting or maximum expulsion efficiency when the flow rate approaches zero and the acceleration level approaches its minimum value consistent with a planar propellant interface.

Flowing Case

A more realistic evaluation of the expulsion efficiency must take into account the effect of flow from the tank in an ac-

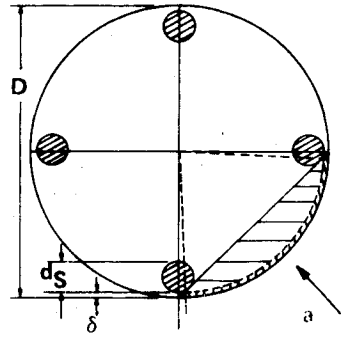

Fig. 3 Nonflowing tank with four-tube device (end view).

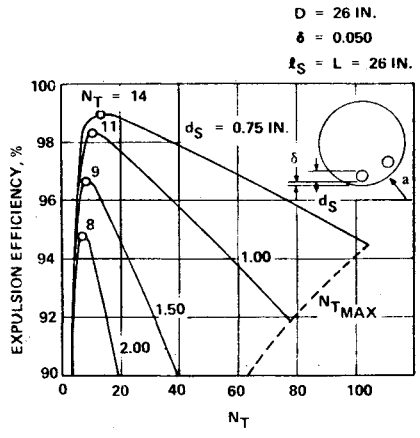

Fig. 4 Expulsion efficiency—nonflowing tank.

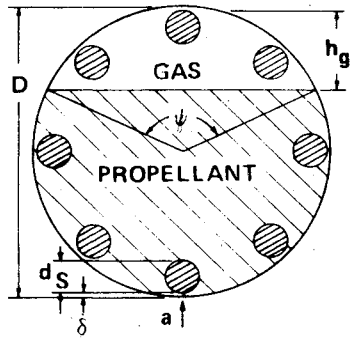

Fig. 5 Flowing tank with eight-tube device (end view).

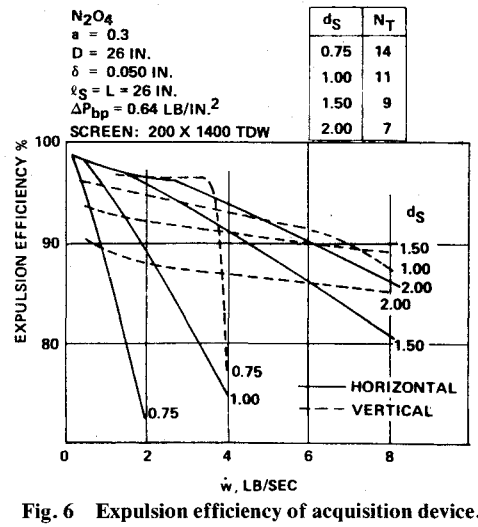

Fig. 6 Expulsion efficiency of acquisition device.

celerating environment and, subsequently, the combined effect of flow pressure losses, static head, and dynamic pressure as it relates to possible screen failure and gas ingestion. These evaluations were made for the nonflowing optimum designs of Fig. 4 in a space environment for both horizontal and vertical positions of the tank.

In the horizontal case, it was assumed that a tube was located at the bottom of the tank, as shown in the eight-tube design of Fig. 5. With the propellant outlet in line with the tank centerline, the flow out of the tank will be equally divided amongst the lower five flowing tubes shown there. From geometry, the expulsion factor in terms of the angle ψ is defined as

$$\mathrm{EF} = \frac{D^2(\psi - \sin\psi)2\pi - N_{nf}d_S^2}{D^2 - N_T\{[4(d_T - t_T) - Nd_h^2]t_T + 4\alpha d_S(1-\phi)t_s\}} \quad (2)$$

and where, from Fig. 5

$$\psi = 2[\cos^{-1}(1 - 2(h_g + \delta)/D)] \quad (3)$$

It should be noted here, as well as in the vertical flowing case to follow, that the expulsion efficiency is defined slightly differently as being the ratio of the quantity of liquid expelled from the tank to the quantity of liquid in the tank initially.

Each of the flowing tubes has a flow pressure loss associated with it; in this case, the loss is the same for each flowing branch as a result of the identical flow rates. This loss consists of the loss through the screen tube itself ΔP_S and the turning and friction losses ΔP_{tf} incurred by the flow in the connecting tubing between the tube and the manifold. The latter was readily computed for a known flow rate from SAE data.[4] The loss across the screen tube was assumed to consist only of the loss through the screen and was computed from Wintec data,[5] assuming a uniform inflow velocity distribution along the tube.

The pressure inside any one of the nonflowing tubes is the total pressure inside the manifold less the pressure due to the hydrostatic head represented by the height of the tube above the gas-liquid interface. Therefore, the greatest pressure differential across the gas-exposed screen surface occurs on the upper surface of the upper tube. Since this pressure differential cannot exceed the screen bubble point value if gas ingestion is to be avoided, the maximum flow rate through each of the flowing tubes can be determined from

$$\Delta P_{bp} = \Delta P_S + \Delta P_{tf} + \rho a h_g \quad (4)$$

The flow dynamic pressure q does not enter into this equation since the manifold pressure is a stagnation pressure based upon a recovered velocity head from the flowing tubes.

The procedure for calculating the expulsion efficiency for a horizontal flowing tank was to pick h_g, calculate ψ from Eq. (3), and then calculate expulsion factor and the corresponding maximum flow rate from Eqs. (2) and (4).

In the vertical case, when the propellant outlet is in the up position, the flow is again equally divided amongst all the tubes. From geometry, the expulsion factor in terms of the tube liquid immersed length ℓ is defined as

$$\mathrm{EF} = \frac{(1 - \ell/\ell_S)(D^2 - N_T d_S^2)}{D^2 - N_T\{[4(d_T - t_T) - Nd_h^2]t_T + 4\alpha d_S(1-\phi)t_s\}} \quad (5)$$

The flow pressure loss for each tube is the sum of two losses. One is the loss ΔP_S which was now calculated over the liquid immersed length rather than the total length of the tube. The second, ΔP_f, considered a friction loss sustained by the liquid in passing through the gas exposed length of the tube, was difficult to determine, due to the unknown nature of the flow within this section of the tube. In this analysis, we assumed that this loss would be directly proportional to the gas exposed length while making a very arbitrary assumption that the loss would be 10% of the dynamic head if the entire length were exposed. The turning and friction losses in the connecting tubing and manifold which entered into Eq. (4) need not be considered here because meniscus failure, when it occurs, will take place at the top of one of the screened tubes.

The static pressure at a point inside the gas-exposed length is the total pressure of the gas less the sum of the flow pressure losses, the pressure due to the hydrostatic head difference between the point and the gas-liquid interface and the dynamic pressure. Thus, the maximum possible flow rate for gas-free expulsion from a tube immersed to a depth ℓ is that satisfying the equation

$$\Delta P_{bp} = \Delta P_S + \Delta P_f + \rho a(\ell_S - \ell) + q \quad (6)$$

The procedure for calculating the expulsion efficiency for the vertical tank was to pick a value of ℓ and then calculate the expulsion factor and the corresponding flow rate from Eq. (5) and (6).

A comparison of the horizontal and vertical expulsion efficiencies of an N_2O_4 tank is shown in Fig. 6 as computed from Eqs. (2)-(6). It shows, for example, that an acquisition device consisting of nine 1.50-in. diameter tubes achieves an expulsion efficiency varying from 92 to 96%, depending upon the attitude, for a flow rate of 2 lb/sec. Since both increasing and decreasing the tube size lowers the overall efficiency defined as an average of the values in both attitudes, this size suggests something of an optimum, at least for the configurations that were studies. It should also be noted that the horizontal attitude was examined under a worst case condition: an acceleration vector which does not exactly bisect the angle between two tubes, a situation which might seldom occur in practice, would result in efficiencies even greater than 96%. We concluded, therefore, that at least to the extent that the analysis was conducted, the multiple screen tube acquisition device demonstrated its feasibility.

Mathematical Model

As stated previously, the screen tube pressure loss term of Eqs. (4) and (6) was based upon an assumed uniform inflow velocity distribution. Because this term can be a significant part of the total pressure drop, as represented by the right side of these equations, a more exact calculation of this loss was needed. The procedure was to assume a more realistic velocity distribution, develop a mathematical model of the flow through the tube, and then calculate the pressure loss based upon this model. If the subsequent test program could be shown to verify this distribution, then the validity of this approach to computing the pressure loss would have been established.

Based upon the large length to diameter ratios of the screen tubes being considered, a significant resistance to the flow entering near the closed end of the tube was anticipated because of the relatively large internal flow pressure drop expected. This suggested that the uniform velocity distribution might better be replaced by a polynomial expression for the velocity in terms of the tube length measured from the closed end. However, based upon the known boundary condition that the flow velocity is zero at the closed end of the tube and that the total integrated flow rate into the tube must equal the known flow rate through the tube, it was shown that only an exponential velocity expression lends itself to a closed form solution. Thus we conveniently assumed an exponential velocity distribution. The following paragraphs described the development of the model based upon this assumption.

The screen tube consists basically of a perforated tube which acts as a support for the pleated screen covering. The intent was to model the flow in sufficient detail to account for all possible losses within the tube. This would not only permit a more exacting calculation of the flow pressure loss but would also provide information on how the design of the tube might be altered, if desired, to make it more suitable for acquisition.

The outer dashed line of the screen tube schematic shown in Fig. 7 is a composite boundary which lumps together the screen, the perforated inner support tube, and the spacing between them. This was done as a matter of convenience because when the velocity (V) distribution is specified, then the losses associated with flow entering the tube through this boundary can be expressed as

$$\Delta P_{cb} = \Gamma_1 V + \Gamma_2 V^2 \tag{7}$$

where Γ_1 and Γ_2 are constants which depend upon the geometry of the composite boundary, propellant properties, and local flow rate. Although the development of these constants is not included here, it was based upon a consideration

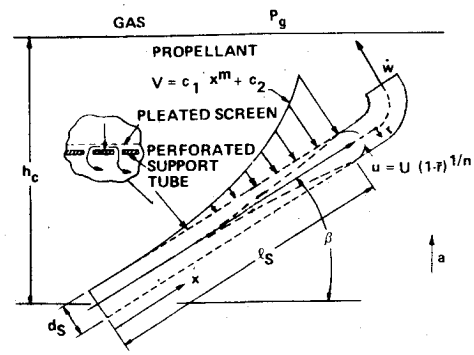

Fig. 7 Schematic of screen tube.

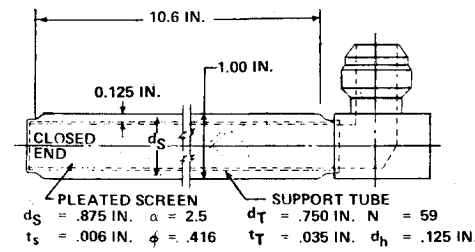

Fig. 8 Screen tube, with dimensions.

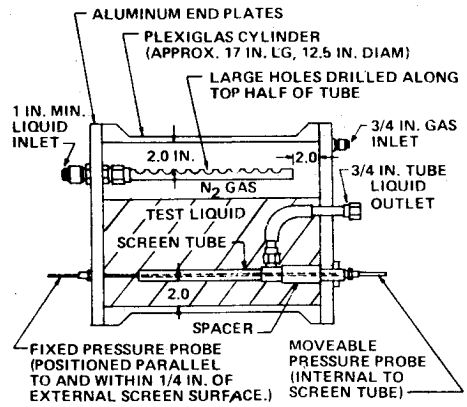

Fig. 9 Screen tube flow test assembly.

of: a) the friction losses through the pleated screen, b) the friction and turning losses between the screen and the holes in the support tube, and c) the friction and expansion losses as a result of flow through the holes of the support tube.

After the flow enters the support tube, it is assumed to come to rest, make a right angle turn, and then accelerate down through the tube. The loss incurred in bringing the flow to rest on the stagnation surface (depicted by the inner dashed line in Fig. 7) is also included in Eq. (7). During its passage from the stagnation surface to the tube exit, the flow is assumed to incur an additional loss due to turbulent mixing ΔP_{tm} with the adjacent streamlines. Thus, the total pressure loss sustained by the fluid in passing through screen tube is

$$\Delta P_S = \Delta P_{cb} + \Delta P_{tm} \tag{8}$$

The exponential velocity distribution, as shown in Fig. 7 and expressed in terms of the axial coordinate, is

$$V = c_1 x^m + c_2 \tag{9}$$

Although shown only on top of the tube, the same distribution is assumed to exist around the periphery. In Eq. (9), the constant c_2 is determined to be zero from the boundary condition that $V=0$ at $x=0$. Equating the in-

tegrated weight flow rate into the tube to the known flow rate determined the constant c_1 such that Eq. (9) with the axial distance nondimensional by ℓ_S becomes

$$V=(m+1)\dot{w}(\bar{x})^m/\rho\pi d_S\ell_S \tag{10}$$

Because of the difficulty of calculating both the composite boundary loss and the turbulent mixing loss in Eq. (8) without knowing the exponential m in Eq. (10), an assumption was made that the two losses could be decoupled, computed separately, and then added to give the total pressure loss. This was done by setting the turbulent mixing loss equal to zero and developing an expression for the total pressure at any point x on the stagnation line in terms of Γ_1, Γ_2, P_g, $\dot{w}$, m, d_S, ℓ_S, a, h_c, and β. Setting the turbulent mixing loss equal to zero is also equivalent to stating that the average total pressure along the stagnation surface is equal to the average total pressure at the open end of the tube. Thus, one obtains the following equation which can be solved for m:

$$\Gamma_1\left[\frac{\dot{w}}{\rho\pi d_S\ell}\right]m+\Gamma_2\left[\frac{\dot{w}}{\rho\pi d_S\ell}\right]^2(m+1)^2\left[\frac{2m}{2m+1}\right]$$

$$-\frac{1}{2\rho g}\left[\frac{4\dot{w}}{\pi(d_T-2t_T)^2}\right]^2+\frac{\rho a\ell}{2}\sin\beta=0 \tag{11}$$

where the immersed length and not the total length of the tube is used. With m determined, the pressure drop through the entire length of the composite boundary was determined to be

$$\Delta P_{cb}=\Gamma_1\left[\frac{\dot{w}}{\rho\pi d_S\ell}\right]+\Gamma_2\left[\frac{\dot{w}}{\rho\pi d_S\ell}\right]^2\frac{(m+1)^2}{2m+1} \tag{12}$$

At this point, the calculations were directed toward determining ΔP_{tm}. From Fig. 7, it is apparent that the streamline entering the tube at $x=\ell_S$ suffers no turbulent mixing loss, while the streamline entering the tube at $x=0$ will suffer the largest loss because it will be in contact with adjacent streamlines the entire length of the tube. Based on these facts, it was reasoned that the average turbulent mixing loss for the entire flowfield should be about one half of the total pressure loss experienced by the centerline streamline. We now postulated that the total pressure loss sustained by the centerline streamline is equivalent to the shear stress experienced by the streamtube whose radius is equal to the Prandtl mixing length and whose axis is the centerline streamline. Then, from Schlichting[6] we determined the total turbulent mixing pressure loss for the flowfield to be

$$\Delta P_{tm}=(\rho/2)(0.14U/n)^2[(.93)\exp 2(n-1)/n]^{-1} \tag{13}$$

In this equation, the centerline velocity U at the open end of the tube can be computed from the Bernoulli equation, once the velocity exponent m is known. The term n is the turbulent velocity exponent (Fig. 7) at the open end of the tube in terms of the radial distance r nondimensionalized by $2(d_T-2t_T)$.

Substituting Eqs. (12) and (13) into Eq. (8) gives the total pressure drop through the screen tube

$$\Delta P_S=\Gamma_1\left[\frac{\dot{w}}{\rho\pi d_S\ell}\right]+\Gamma_2\left[\frac{\dot{w}}{\rho\pi d_S\ell}\right]^2\frac{(m+1)^2}{2m+1}$$

$$(\rho/2)(0.14U/n)^2[(.93)\exp 2(n-1)/n]^{-1} \tag{14}$$

A computer program of the above model was set up to compute this ΔP_S as well as V vs x.

III. Test Program

The twofold purpose of the test program was: a) to verify the assumed exponential velocity distribution along the screen tube, and b) to demonstrate the feasibility of a multiple tube acquisition device in a full scale tank. The following paragraphs describe the test apparatus, test procedures, and results obtained from the 1 g test program.

Table 1 Flow test results, horizontal tube

Water $\beta=0°$ $a=1$ $\ell_S=10.6$ in.			
$\dot{w}$ (lb/sec)	$\bar{x}$	ΔP (in.H_2O)	Δp (in.H_2O)
0.5	0.056	2.4	3.0
	0.245	2.4	3.5
	0.434	2.2	3.5
	0.623	2.2	3.9
	0.811	2.1	4.5
	1.0	2.0	7.3
1.0	0.056	3.3	4.0
	0.245	3.3	5.1
	0.434	3.2	5.3
	0.623	3.0	6.1
	0.811	3.0	8.5
	1.0	2.8	19.3
1.5	0.056	4.1	5.8
	0.245	3.9	6.5
	0.434	3.8	6.9
	0.623	3.7	8.1
	0.811	3.5	12.7
	1.0	3.4	39.4
2.0	0.056	4.5	7.8
	0.245	4.5	8.1
	0.434	4.3	8.0
	0.623	4.1	10.1
	0.811	3.9	16.6
	1.0	4.1	65.8

Table 2 Flow test results, vertical tube

Freon T.F. $\beta=90°$ $a=1$ $\ell_S=10.6$ in.	
$\dot{w}$ (lb/sec)	ℓ_{min} (in.)
0.56	5.4
0.74	6.5
0.88	7.6
0.97	8.9

Screen Tube

A sketch of the screen tube used in these tests is shown in Fig. 8, along with the pertinent dimensions. It consists of a perforated stainless steel inner support tube wrapped externally with a stainless steel 200×1400 twilled dutch weave screen (15 micron absolute rating) with longitudinal pleats about 1/8 in. deep.

Figure 9 is a schematic of the test assembly in which the tube was flow tested. A basic requirement of the test fixture assembly was that the screen tube be rigidly mounted away from the shell wall and relatively remote from the liquid inlet. Such a position would guarantee that flow into the tube would be uniform and symmetrical around the circumference when tested, since these conditions were assumed in the mathematical model.

The tests were conducted with the test fixture positioned either horizontally or vertically. The tank was partially filled with liquid so that the tube was partially or completely immersed in the liquid, depending upon the attitude. Then the system was pressurized with nitrogen and the rate of liquid expulsion measured with a flowmeter. During the expulsion, the tank was pressure filled with liquid so as to maintain a constant immersion depth.

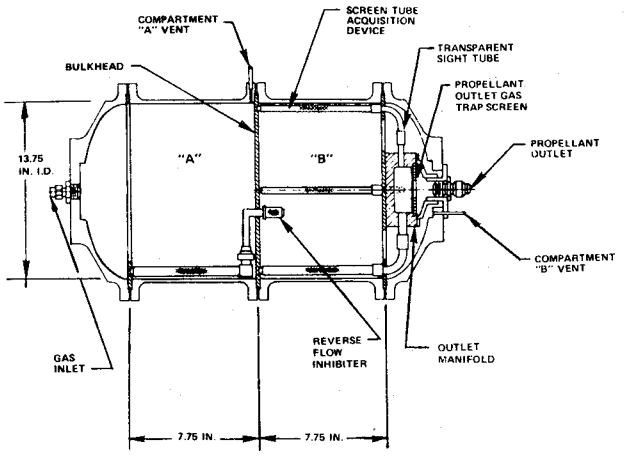

Fig. 10 Test tank.

Pressure measurements were made both internally and externally to the tube during an expulsion using 3/16-in. o.d. stainless steel probes. The outside probe was located 1/4 in. from the surface of the tube at the closed end. Because of the low flow velocity there, it essentially measured the total pressure. At the same time either of two similar movable probes was used to measure the total or static pressure inside the tube at various axial stations. These measurements were all read as pressure differentials in a liquid manometer using the same liquid as in the test chamber.

The tests with the screen tube in a horizontal position were performed using distilled water. Results are shown in Table 1 for flow rates of 0.5-2.0 lb/sec in terms of the nondimensionalized distance from the closed end ($\bar{x}=0$) of the tube. The pressure differentials shown there are the values of the total pressure at the outer probe minus either the total or static pressure of the movable inner probe, as the case may be.

Difficulty in achieving a repeatable bubble point value for water on stainless steel screen material prompted the use of Freon T.F. for expulsion tests in the vertical position. Results are shown in Table 2 as the minimum tube immersed length at which screen failure and gas ingestion occurred for a given flow rate.

Test Tank

A two-compartment cylindrical tank with ellipsoidal heads was built to test the feasibility of using screen tubes as an acquisition device. It was a one half scale model of a full size N_2O_4 tank designed to operate in a space environment ($a=0.3$) and have an expulsion efficiency of at least 98% in the second compartment at flow rates up to 1.00 lb/sec. This performance was based upon a screen bubble point value of 0.64 psi for N_2O_4. To simulate this condition in the laboratory tests ($a=1$) using water required that the test tank be capable of flowing a maximum of 1.25 lb/sec without screen failure and gas ingestion.

A sketch of the test tank is shown in Fig. 10. Compartment A is presumably sized to meet the propellant demand during an initial phase of a space mission when the acceleration vector is known. The single screen tube acquisition device shown there was purposely located at the bottom of the tank relative to this vector. Compartment B must satisfy the propellant demand in space when the acceleration is small and randomly oriented. If the tank geometry and test conditions had been identical with those investigated in the analysis (Fig. 6), then eleven, 1.00 in. diameter tubes would have been required in compartment B for an optimum explusion efficiency of about 95.5% in both attitudes. Since a simpler design would serve to demonstrate feasibility, only four tubes were used in the compartment B acquisition device.

The single acquisition tube in compartment A and the one at the same 6 o'clock position (in an end view of the tank) in compartment B were 1.00 in. diameter tubes like that shown in Fig. 8, except they were shorter (6.72 in.). The remaining tubes in compartment B at the 9, 12, and 3 o'clock positions were slightly smaller in diameter (0.625 in.) The tube in compartment A was connected to a small screen tube at the bulkhead in compartment B. This small tube serves to prevent a reverse flow from compartment B into compartment A after the latter has been partially emptied. The four tubes in compartment B were connected to an outlet manifold containing a screen near the tank outlet which serves as a gas trap. The tank shell was fabricated of plexiglas and the connecting passages were made of Tygon tubing to permit observation of the flow process.

The tank was flow tested in both the horizontal and vertical positions. Prior to a test both compartments were filled with water while the tank was in an upright position (propellant outlet up). The test started by introducing nitrogen gas into compartment A, forcing the liquid through the tube there and through the bulkhead reverse flow inhibitor tube and then into compartment B. Liquid continued to flow until compartment A was empty or until the pressure differential across the gas exposed screen surface exceeded the screen bubble point. When this occurred, gas penetrated into compartment B and forced the liquid through the submerged tubes into the outlet manifold, through the gas trap screen, and out the discharge port. Similarly, liquid continued to flow in compartment B in the absence of gas entrainment until the screen bubble point was exceeded. For each test, the expulsion rate was computed from the measured weight of expelled water and the expulsion time. Visual observations were made of the expulsion efficiency.

Test flow rates up to 1.43 lb/sec in the horizontal position gave expulsion efficiencies greater than 98% in compartment B and 99% in compartment A. Vertical expulsions, which obviously prevent compartment A from completely emptying, resulted in expulsion efficiencies greater than 95% in compartment B at flow rates up to 1.20 lb/sec. These flow rates were not the maximum obtainable since in either instance screen failure had not yet occurred.

IV. Comparison of Analytical and Test Results

Analytical calculations of V and ΔP_S for different flow rates were made using Eqs. (10) and (14) and the results compared with the test results of Table 1 for a horizontal tube. Before calculating V and ΔP_S, m was calculated from Eq. (11) after determining the composite boundary loss coefficients Γ_1 and Γ_2. Both of these coefficients are dependent upon the boundary geometry and the propellant properties. In addition, Γ_1 includes the loss through the screen which is dependent upon the local velocity, making it a function of the length along the tube while Γ_2 is a constant.

It was obvious that, since Γ_1 is a function of the very velocity we wished to determine, it would have to be determined by some approximate means. This was done by assuming a constant velocity distribution along the tube and then computing a resistance coefficient for the screen based upon this distribution. The resistance coefficient denoted as k is the ratio of the pressure drop to the unit flow rate through the screen and was computed as the slope of the 200×1400 TDW curve in the Wintec data.[5] This curve had to be extrapolated to the lower unit flow rates considered in this study. Selecting a flow rate (1.5 lb/sec) we determined that, depending upon the type of extrapolation, k could vary from 2.1 to 4.6. At this point it was decided to determine what value of k would be required to make the computed value of ΔP_S for a given flow rate be equal to the measured value of a horizontally ($\beta=0°$) flowing tube from Table 1. Choosing a flow rate of 1.5 lb/sec and noting that the loss measured at the open end ($\bar{x}=1$) of the tube should represent the total loss through the tube, then, from Table 1, $\Delta P_S=3.4$ in. H_2O (0.122 psi). With this as the pressure loss, k was found to be

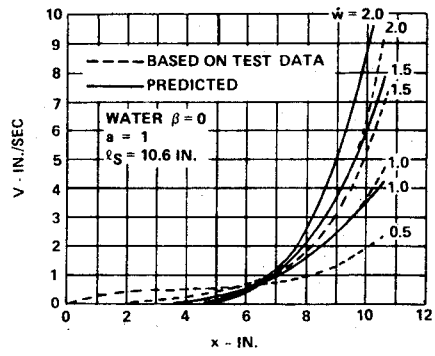

Fig. 11 Inflow velocity profile along tube surface.

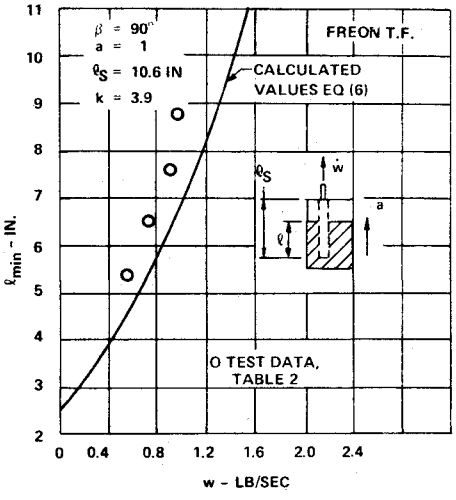

Fig. 12 Liquid height at screen failure.

3.9 and m was calculated to be 4.7 from Eq. (11). As a matter of interest, this same value of k was used to calculate ΔP_S for the other flow rates. When this was done, the results indicated a more rapid increase in the pressure drop with increasing flow rate than what was observed in the tests.

The pressure differentials in Table 1 denote pressures at the internal moving total and static probes, which are less than those at the other reference probe. For a turbulent mixed flow, the quantity $\Delta p - \Delta P$ should represent the average dynamic head inside the tube. With this quantity an average value of the flow velocity u' at a given station was calculated using the Bernoulli equation. From the plot of u' vs x, we determined the change in inflow velocity over an incremental length of tube from mass continuity considerations using

$$\Delta V = \{ [(d_T - 2t_T)^2 - d_p^2] / 4d_T \} \, \Delta u' / \Delta x \qquad (15)$$

This equation was used to determine V vs x. Figure 11 shows the results (dashed lines) of applying the above procedure to obtain the inflow velocity profile for the different flow rates using this procedure. The solid lines are the corresponding profiles as predicted by the model. A comparison of these curves show that the incoming velocity profile is indeed exponential, especially at the higher flow rates ($\dot{w} > 1.0$). At the lower flow rates ($\dot{w} \leq 1.0$), it apparently deviates from this form.

Table 3 shows the computed values of m and n for the predicted curves of Fig. 11. It is seen that m increases with increasing flow rate as one would expect. Thus at least for the length to diameter ratio $\ell_S/d_S = 1..8$ of the tube tested, an ever increasing length of the tube becomes ineffective in flowing liquid as the flow rate increases. This too was borne out by the test results. The computed values of n which are larger than

Table 3 Analytical constants

$\dot{w}$	m	n
0.5	2.09	7.98
1.0	3.59	13.82
1.5	4.67	18.63
2.0	5.47	22.63

Table 4 Expulsion efficiencies in compartment B

		Expulsion efficiency (%)	
Attitude	$\dot{w}$(lb/sec)	Calculated	Test
Horizontal	1.43	98.5	98+
Vertical	1.20	88.0	95+

those associated with turbulent flow ($n = 7$) indicated the existence of a rather flat velocity profile at the open end of the tube at the higher flow rates.

Flow tests with the tube in a vertical position ($\beta = 90°$) also verified the exponential velocity profile. These tests also substantiated the calculated results showing that m decreases (inflow velocity distribution flattens) as the ratio of the immersed length to diameter ratio decreases. Using Eq. (14) to calculated ΔP_S in Eq. (6) and then computing the minimum value of ℓ from this equation, we obtained the results shown in Fig. 12. The differences shown there between these values and the measured results of Table 2 cannot be attributed to an inadequacy of the model because the ΔP_S is very small relative to the static head represented by the gas exposed length of the tube and the flow dynamic pressure, both of which enter into the calculation of $\ell_{\min}$ in addition to ΔP_S. Rather, the differences is suspected as being the result of accelerating flow within the gas exposed part of the tube (as indicated by pressure measurements) and not a constant flow velocity, as was assumed in the calculations.

Since the results of the expulsion tests could not be compared with the results of Fig. 6, additional calculations of the expulsion efficiency for the test conditions were made using Eqs. (2)-(6) and a bubble point value of 1.74 psi for water. These results are shown in Table 4 along with the test results. These efficiencies, which are for compartment B only, show excellent agreement for the horizontal position. For the vertical position the observed performance was considerably greater than that predicted. This is believed to be partly the result of the fact that the model calculates what appears to be unusually large values for the turbulent mixing loss at very small immersed length to diameter ratios. Another factor in this difference is the presence of a meniscus at the intersection of the gas-liquid interface and the tubes. It has the effect of increasing the flow area into the tube, delaying screen failure, and permitting more liquid to be expelled than would be the case in its absence.

V. Conclusions

The exponential velocity distribution assumed in the mathematical model was verified by tests in both the horizontal (Fig. 11) and vertical positions of the tube. Both the model and the test results show that the velocity exponent m increases with increasing flow rate and decreases with decreasing immersed length to diameter ratio. Although the test data verified the model, the tube pressure drop values calculated using this model showed a greater increase with increasing flow rate than what was actually observed during the tests. The present model would be expected to show greater correspondence with test data if a velocity dependent k were used rather than a constant value. This would be possible through an iterative procedure and should be considered in any future applications of the model.

In exceeding the required flow rate of 1.25 lb/sec from a horizontally positioned test tank without incurring gas ingestion, we demonstrated the feasibility of the pleated screen tube acquisition device in achieving an expulsion efficiency of at least 98% in a full scale N_2O_4 tank in a space environment. Not intended as an optimum design, the addition of tubes to the existing acquisition device would almost certainly increase the expulsion efficiency to this level in the vertical position as well for both space and test conditions.

References

[1]Dowdy, M.W. and DeBrock. S.C., "Selection of a Surface Tension Propellant Management System for the Viking 75 Orbiter," *Journal of Spacecraft and Rockets,* Vol. 10, No. 9, Sept. 1973, pp. 549-558.

[2]Vote, F.C. and Schatz, W.J., "Development of the Propulsion Subsystem for the Viking 75 Orbiter," AIAA Paper 73-1208, Las Vegas, Nev., Nov. 1973.

[3]Park, L.T., Corgin, J.D., and Ernst, R.D., "Titan Transtage Spacecraft Propulsion System," AIAA Paper 73-1210, Las Vegas, Nev., Nov. 1973.

[4]*Aero-Space Applied Thermodynamics Manual,* Society of Automotive Engineers, Warrendale, Pa., Feb. 1960, Figs. 1A-4 and 1A-9.

[5]"Cryogenic Filter Study," Wintec Corp., Los Angeles, Calif., 1973, Figure 3.

[6]Schlichting, H., *Boundary Layer Theory*, McGraw Hill, New York City, 1960, Eqs. (20.16) and (20.18).